

# On the applicability of the Rayleigh approximation for coated spheroids in the near-infrared

V.V. Somsikov and N.V. Voshchinnikov

Astronomical Institute, St. Petersburg University, Bibliotechnaya pl. 2, 198904 St. Petersburg-Peterhof, Russia

Received 27 July 1998 / Accepted 9 December 1998

**Abstract.** Calculations of the extinction and polarization profiles in the wavelength range  $\lambda$  2.7–22  $\mu\text{m}$  have been performed for silicate core – icy mantle spheroidal grains using the exact solution to the light scattering problem and the Rayleigh approximation.

It is concluded that the 10% accuracy of the Rayleigh approximation is guaranteed in the case of extinction (polarization) if the particle size does not exceed  $r \lesssim 1.15 \mu\text{m}$  (1.10  $\mu\text{m}$ ), 0.85  $\mu\text{m}$  (0.35  $\mu\text{m}$ ), 0.25  $\mu\text{m}$  (0.15  $\mu\text{m}$ ) within the 18  $\mu\text{m}$ , 10  $\mu\text{m}$  and 3  $\mu\text{m}$  bands respectively, where  $r$  is the radius of a sphere with the same volume as a spheroid.

**Key words:** infrared: ISM: lines and bands – ISM: dust, extinction – polarization – scattering

## 1. Introduction

Absorption dusty bands are found in the infrared (IR) spectra of protostellar objects and some stars embedded in molecular clouds (Willner et al. 1982; Whittet 1992). They are attributed to silicates and various ices ( $\text{H}_2\text{O}$ ,  $\text{NH}_3$ ,  $\text{CO}$ ,  $\text{CH}_3\text{OH}$ ,  $\text{CO}_2$ , etc.). The profiles and relative strengths of the bands vary significantly from object to object. In a few cases, the linear polarization inside the bands was measured (Aitken et al. 1988, 1989; Hough et al. 1989, 1996).

The observations can be explained most naturally in the frame of the dichroic absorption of light by aligned non-spherical dust grains consisting of a refractory core and volatile mantle. Such a model is popular and has been applied to the interpretation of the water ice and silicate bands (Lee & Draine 1985), the 9.7 and 18  $\mu\text{m}$  silicate features (O’Donnell 1994), the bands of solid CO (Tielens et al. 1991), OCS (Palumbo et al. 1995),  $\text{H}_2\text{O}$  (Hough et al. 1996) and  $\text{CH}_4$  (Boogert et al. 1997). In all cases, the authors used the model of confocal core-mantle spheroids. The optical properties of particles were calculated in the Rayleigh approximation (see Draine & Lee 1984 for details).

The applicability of the Rayleigh (electrostatic) approximation depends on two conditions (van de Hulst 1957; Bohren & Huffman 1983):

$$\frac{2\pi}{\lambda}(\text{size}) \ll 1 \quad (1)$$

and

$$|m| \frac{2\pi}{\lambda}(\text{size}) \ll 1, \quad (2)$$

where  $m$  is the complex refractive index of the material and  $\lambda$  is the wavelength of radiation. Because the refractive index increases within the bands, the same accuracy of the Rayleigh approximation in a band and a neighboring continuum can be reached for particles of smaller sizes in the band. On the other hand, the dust grains seem to be expected to be large in molecular regions, which makes the use of the Rayleigh approximation for modelling the absorption bands quite questionable.

In this paper, we estimate the accuracy of the Rayleigh approximation for calculations of the IR extinction and polarization profiles observed in the wavelength range  $\lambda$  2.7–22  $\mu\text{m}$  using the exact solution to the light scattering problem for core-mantle spheroids.

## 2. Exact solution and Rayleigh approximation

The optical properties of a core-mantle spheroid can be calculated if we specify its type (prolate or oblate) and define the values of the core and mantle refractive indices, the ratios of the major semiaxis to the minor one for core  $a_2/b_2$  and mantle  $a_1/b_1$ , particle size and the angle  $\alpha$  between the directions of the incident radiation and the rotation axis of spheroid. As the size of a spheroid, we choose the radius of the equivolume sphere  $r$ . It follows from

$$r^3 = a_1 b_1^2 \quad \text{for prolate spheroids} \quad (3)$$

and

$$r^3 = a_1^2 b_1 \quad \text{for oblate ones.} \quad (4)$$

The exact solution to the light scattering problem for coated spheroids by the separation of variables method was obtained by Farafonov (1994) and described by Farafonov et al. (1996) in detail. The solution is valid for confocal spheroids, that means the core aspect ratio has to exceed the mantle one,  $a_2/b_2 > a_1/b_1$ . Note that the thickness of the mantle is not constant across the surface of a confocal coated spheroid: it is maximal along the

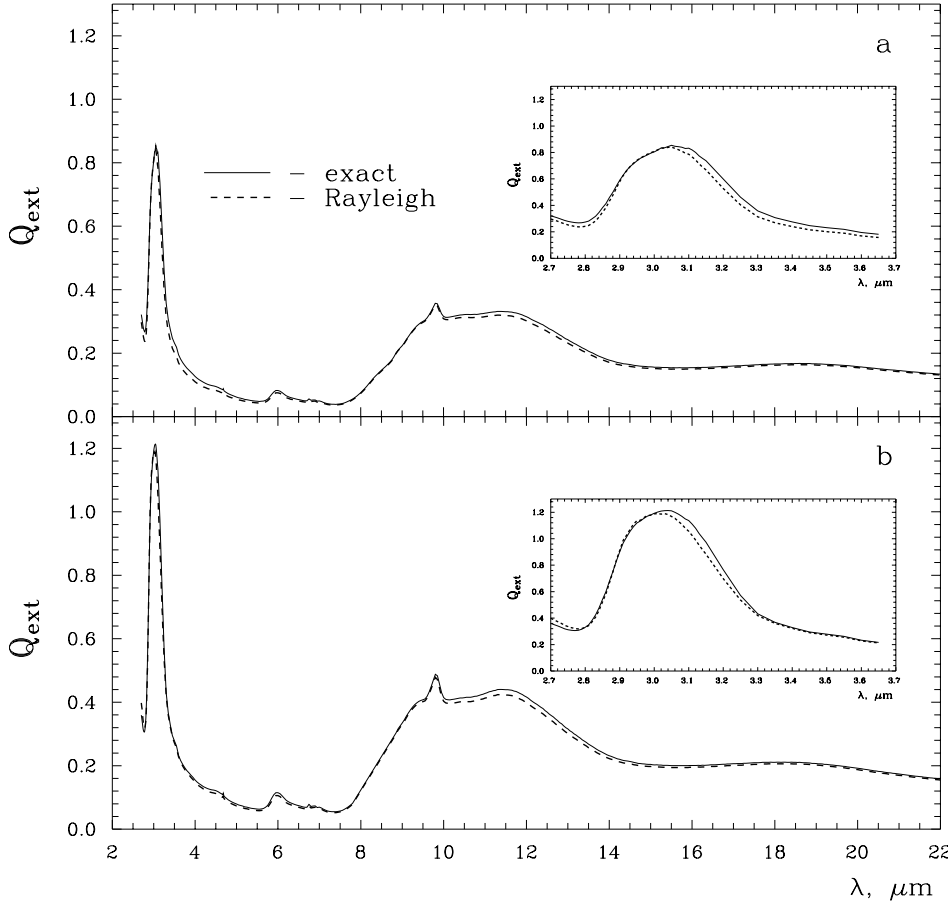


**Fig. 1a and b.** The extinction efficiency factors  $Q_{\text{ext}}$  for prolate **a** and oblate **b** core-mantle spheroids;  $a_1/b_1 = 2$ ,  $r = 0.5 \mu\text{m}$ ,  $\alpha = 90^\circ$ ,  $V_{\text{core}}/V_{\text{total}} = 0.5$

minor axis and minimal along the major one, i.e. in all cases  $\Delta a = a_1 - a_2 < \Delta b = b_1 - b_2$  (Farafonov & Voshchinnikov 1997).

In astrophysical applications, it is more convenient to introduce the ratio of the core volume to the total volume of a coated particle. This ratio can be found using the semiaxes ratios as

$$\frac{V_{\text{core}}}{V_{\text{total}}} = \left( \frac{a_2/b_2}{a_1/b_1} \right)^{k+1} \left[ \frac{(a_1/b_1)^2 - 1}{(a_2/b_2)^2 - 1} \right]^{3/2}, \quad (5)$$

where  $k = 0$  for prolate spheroids and  $k = 1$  for oblate ones.

We assume that the incident radiation is non-polarized. Then the extinction and polarization profiles are determined by the wavelength dependencies of the extinction  $Q_{\text{ext}}(\lambda)$  and polarization  $Q_{\text{pol}}(\lambda)$  efficiency factors

$$Q_{\text{ext}}(\lambda) = \frac{Q_{\text{ext}}^{\text{TM}}(\lambda) + Q_{\text{ext}}^{\text{TE}}(\lambda)}{2}, \quad (6)$$

$$Q_{\text{pol}}(\lambda) = \frac{Q_{\text{ext}}^{\text{TM}}(\lambda) - Q_{\text{ext}}^{\text{TE}}(\lambda)}{2}. \quad (7)$$

Here, the superscript TM (TE) is related to the case when the electric vector  $\mathbf{E}$  of the incident radiation is parallel (perpendicular) to the plane defined by the rotation axis of a spheroid and the wave vector.

Expressions for the factors  $Q_{\text{ext}}^{\text{TM,TE}}$  can be found in the paper of Farafonov et al. (1996). Formulae for the factors using the Rayleigh approximation are given by Draine & Lee (1984).

### 3. Results and discussion

We compared the factors  $Q_{\text{ext}}$  and  $Q_{\text{pol}}$  for core-mantle prolate and oblate spheroids with aspect ratios  $a_1/b_1 = 2$  and 5, volume ratios  $V_{\text{core}}/V_{\text{total}} = 0.1, 0.5, 0.9$  and several values of the sizes  $r$  for two cases of orientation ( $\alpha = 0^\circ$  and  $90^\circ$ ). The calculations were carried out in the wavelength range  $\lambda \lambda 2.7 - 22.0 \mu\text{m}$ . The ‘‘astronomical’’ silicate (Laor & Draine 1993) was taken as the core material, and the ‘‘weak interstellar mixture’’ at 10 K (Hudgins et al. 1993) as the mantle one.

We found the wavelength dependence of the percent deviations of the efficiency factors calculated in the Rayleigh approximation  $Q_{\text{ext}}^{\text{Ray}}$  from those obtained with the exact solution  $Q_{\text{ext}}^{\text{exact}}$

$$\Delta_{\text{ext}}(\lambda) = \frac{Q_{\text{ext}}^{\text{exact}}(\lambda) - Q_{\text{ext}}^{\text{Ray}}(\lambda)}{Q_{\text{ext}}^{\text{exact}}(\lambda)} \cdot 100\%. \quad (8)$$

A similar equation can be written for  $\Delta_{\text{pol}}$ .

The results are presented in Tables 1, 2 and Figs. 1–3. First of all, we concentrate on the discussion of the  $3 \mu\text{m}$  water ice band and silicate bands. The values of  $\Delta_{\text{ext}}$  and  $\Delta_{\text{pol}}$  in Tables 1, 2 are given for three wavelengths ( $3 \mu\text{m}$ ,  $9.5 \mu\text{m}$ ,  $18.5 \mu\text{m}$ ) which are close to the central positions of the  $\text{H}_2\text{O}$  and silicate bands in the case of small particles consisting of the pure material of the mantle or core.

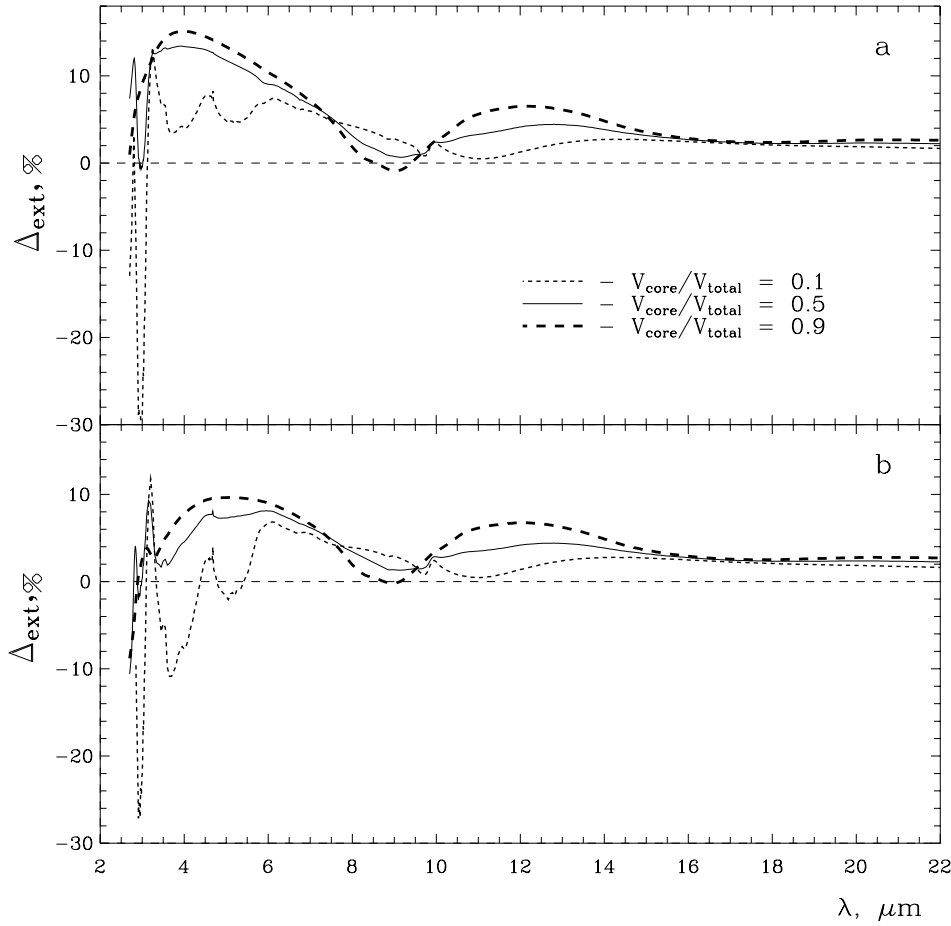


**Fig. 2a and b.** Relative difference between the exact and Rayleigh extinction efficiency factors  $\Delta_{\text{ext}}$  for prolate **a** and oblate **b** core-mantle spheroids;  $a_1/b_1 = 2$ ,  $r = 0.5 \mu\text{m}$ ,  $\alpha = 90^\circ$ ; the values of  $V_{\text{core}}/V_{\text{total}}$  are indicated

### 3.1. The $\text{H}_2\text{O}$ and silicate bands

#### 3.1.1. Extinction profiles

Fig. 1 shows the extinction efficiency factors  $Q_{\text{ext}}^{\text{exact}}$  and  $Q_{\text{ext}}^{\text{Ray}}$  for prolate and oblate spheroids with  $r = 0.5 \mu\text{m}$ . At first sight, the behaviour of the profiles is similar. However, on a larger scale it is seen that the profiles calculated according to the exact solution are broader and their maxima are shifted to longer wavelengths. Thus, the use of the Rayleigh approximation mainly leads to a deformation of the red wing of the profiles. Although the exact and approximate factors differ less than 1% at  $\lambda = 3 \mu\text{m}$  (see Table 1),  $\Delta_{\text{ext}}$  may exceed 10% at  $\lambda = 4\text{--}6 \mu\text{m}$  (Fig. 2a).

The wavelength dependence of  $\Delta_{\text{ext}}$  plotted in Fig. 2 demonstrates that the errors induced by the Rayleigh approximation are not constant within the bands and depend on the volume ratio  $V_{\text{core}}/V_{\text{total}}$ . Note that if  $\alpha = 0^\circ$ , the radiation propagates along the major axis of a prolate spheroid and along the minor axis of an oblate spheroid. If  $\alpha = 90^\circ$ , the situation changes. But in both cases  $\Delta b > \Delta a$ , i.e. the mantles of prolate spheroids shown in Figs. 1, 2 are thicker than those of oblate ones with the same values of  $V_{\text{core}}/V_{\text{total}}$ . However, as it is seen from Figs. 2a and 2b, at several wavelengths the values of  $\Delta_{\text{ext}}$  for spheroids with thinner mantles (oblate) exceed those for spheroids with thicker mantles (prolate).

From the results presented in Table 1 it follows that the differences between the “exact” and “Rayleigh” extinction profiles do not change significantly with the particle orientation, shape (the aspect ratio  $a_1/b_1$ ) and type (prolate/oblate). Strong variations are only due to the changes of the particle size and the ratio  $V_{\text{core}}/V_{\text{total}}$  (Table 1, Fig. 2).

The values of  $\Delta_{\text{ext}}$  are given in Table 1 at three fixed wavelengths, but it is also of interest to find a maximum of  $\Delta_{\text{ext}}$  within each band. For the particles with  $r = 0.1 \mu\text{m}$ , the values of  $\Delta_{\text{ext}}$  do not exceed 2.6%, 0.2% and 0.1% for the  $3 \mu\text{m}$ ,  $9.7 \mu\text{m}$  and  $18 \mu\text{m}$  bands, respectively. Even when the size becomes as large as  $r = 1.0 \mu\text{m}$ , the difference between the exact and approximate results remains less than 10% inside the  $18 \mu\text{m}$  band.

For practical purposes, it is interesting to evaluate the size of the particles for which  $\Delta_{\text{ext}} < 10\%$ . We find that this occurs for both prolate and oblate spheroids if  $r \lesssim 0.25 \mu\text{m}$  in the  $3 \mu\text{m}$  band,  $r \lesssim 0.85 \mu\text{m}$  in the  $10 \mu\text{m}$  band and  $r \lesssim 1.15 \mu\text{m}$  in the  $18 \mu\text{m}$  band.

#### 3.1.2. Polarization profiles

The wavelength dependence of the polarization efficiency factors  $Q_{\text{pol}}^{\text{exact}}$  and  $Q_{\text{pol}}^{\text{Ray}}$  is plotted in Fig. 3 for the prolate and oblate spheroids with  $r = 0.5 \mu\text{m}$ . In Table 2, the relative dif-

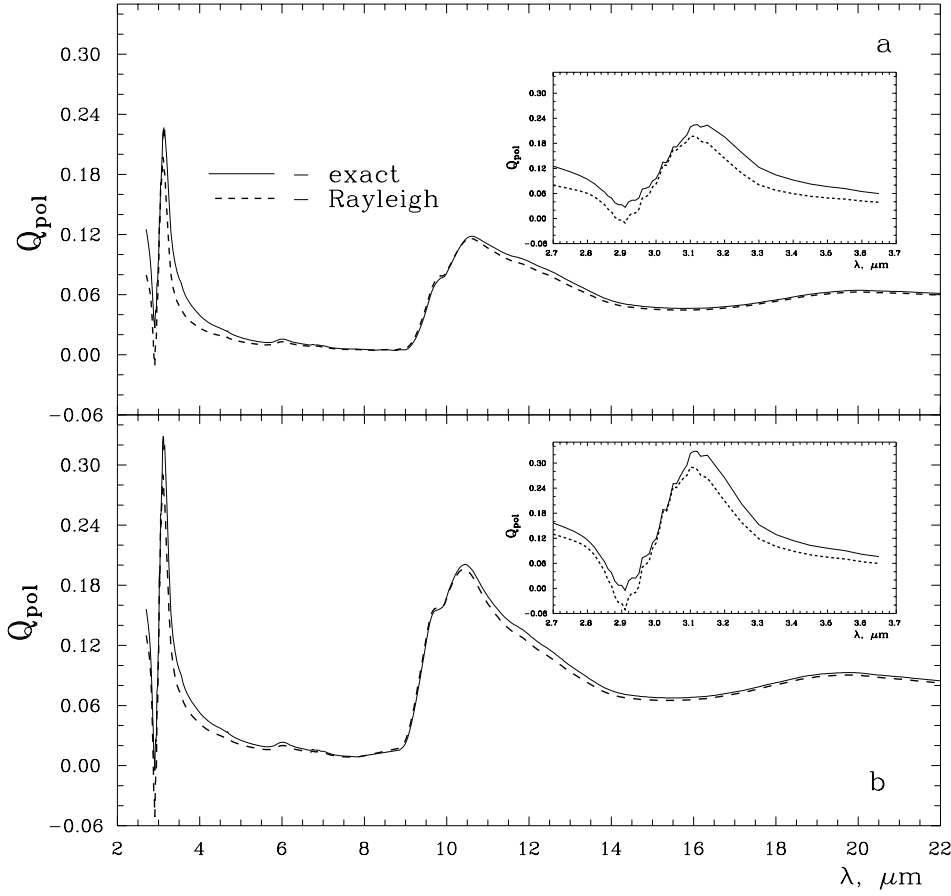


**Fig. 3a and b.** The same as Fig. 1 but now for the polarization efficiency factors  $Q_{\text{pol}}$

**Table 1.** Relative difference between the exact and Rayleigh extinction efficiency factors  $\Delta_{\text{ext}}$  for core-mantle spheroids

$a_1/b_1$	$r, \mu\text{m}$	$V_{\text{core}}/V_{\text{total}}$	$\alpha = 0^\circ$			$\alpha = 90^\circ$			
			$3 \mu\text{m}$	$9.5 \mu\text{m}$	$18.5 \mu\text{m}$	$3 \mu\text{m}$	$9.5 \mu\text{m}$	$18.5 \mu\text{m}$	
Prolate spheroid									
2.0	0.10	0.10	1.20%	0.12%	0.09%	1.04%	0.08%	0.09%	
		0.50	1.83	0.17	0.10	1.76	0.09	0.10	
		0.90	2.38	0.20	0.12	2.57	0.11	0.11	
	0.30	0.50	8.50	1.29	0.91	8.50	0.60	0.85	
	0.50	0.50	1.98	2.89	2.44	-0.44	0.97	2.24	
5.0	1.00	0.50	-122.0	3.75	8.33	-214.0	-3.89	7.31	
	0.10	0.50	1.54	0.15	0.09	1.49	0.04	0.08	
	0.30	0.50	5.17	1.13	0.75	5.06	0.18	0.66	
	0.50	0.50	-2.20	2.44	1.98	-12.4	-0.16	1.66	
Oblate spheroid	2.0	0.10	0.10	0.82	0.07	0.08	1.04	0.08	0.09
			0.50	1.73	0.07	0.10	1.81	0.11	0.10
			0.90	2.58	0.11	0.11	2.49	0.15	0.11
	0.30	0.50	8.47	0.40	0.83	8.54	0.77	0.88	
	0.50	0.50	-0.59	0.38	2.18	0.33	1.48	2.33	
	1.00	0.50	-250.0	-6.71	7.14	-154.0	-1.31	7.75	
	5.0	0.10	0.50	1.53	0.02	0.08	1.57	0.05	0.08
		0.30	0.50	5.48	-0.09	0.65	5.43	0.20	0.70
		0.50	0.50	-13.4	-0.94	1.66	-8.08	-0.04	1.80
1.00		0.50	-334.0	-10.7	4.74	-166.0	-6.00	5.29	

**Table 2.** Relative difference between the exact and Rayleigh polarization efficiency factors  $\Delta_{\text{pol}}$  for core-mantle spheroids ( $\alpha = 90^\circ$ )

$a_1/b_1$	$r, \mu\text{m}$	$V_{\text{core}}/V_{\text{total}}$	$3 \mu\text{m}$	$9.5 \mu\text{m}$	$18.5 \mu\text{m}$
Prolate spheroid					
2.0	0.10	0.10	-0.70%	-0.02%	0.11%
		0.50	2.59	-0.21	0.12
		0.90	4.63	-0.24	0.13
	0.30	0.50	14.3	-2.39	0.98
		0.50	13.3	-8.31	2.50
5.0	0.10	0.50	-317.0	-64.4	7.58
		0.50	2.47	-0.21	0.09
	0.30	0.50	11.8	-2.30	0.74
		0.50	1.20	-7.66	1.82
		0.50	-393.0	-47.6	4.53
Oblate spheroid					
2.0	0.10	0.10	-0.47	0.05	0.11
		0.50	2.35	-0.05	0.11
		0.90	4.50	-0.06	0.13
	0.30	0.50	12.0	-0.80	0.98
		0.50	8.72	-3.38	2.53
5.0	0.10	0.50	-198.0	-28.3	7.96
		0.50	2.11	-0.04	0.09
	0.30	0.50	7.62	-0.67	0.77
		0.50	-6.62	-2.69	1.94
		0.50	-280.0	-18.3	5.45

ferences between the polarization efficiency factors  $\Delta_{\text{pol}}$  are given at three wavelengths.

In general, the conclusions made for the extinction profiles are valid for the case of polarization too: a strong dependence on the particle size and the core/mantle volume ratio and a weak dependence on other parameters. The exact theory also leads to broader profiles with the maxima shifted to longer wavelengths (see Fig. 3). The largest deviations are in the red wing of the profile. Note that the reversal of polarization in the blue wing of the  $3 \mu\text{m}$  band obtained in the Rayleigh approximation disappears if we apply the exact theory.

It should be emphasized that the Rayleigh approximation can lead to large errors for polarization. This is because of the small values of the polarization efficiency factors  $Q_{\text{pol}}$  which may vanish in the absorption bands (see Eq. (8)).

The maximum values of  $\Delta_{\text{pol}}$  in the silicate bands are of the same order as those of  $\Delta_{\text{ext}}$ . Another situation occurs within the  $3 \mu\text{m}$  band where  $\Delta_{\text{pol}}$  can be very large.

As for the particle size for which  $\Delta_{\text{pol}} < 10\%$  this occurs if  $r \lesssim 0.15 \mu\text{m}$  in the  $3 \mu\text{m}$  band,  $r \lesssim 0.35 \mu\text{m}$  in the  $10 \mu\text{m}$  band and  $r \lesssim 1.10 \mu\text{m}$  in the  $18 \mu\text{m}$  band.

### 3.2. Other bands

In the previous discussion, we considered mantles consisting of “weak interstellar mixture”. This sample contains about 90% of water ice (Hudgins et al. 1993). Therefore, the  $3 \mu\text{m}$  band of  $\text{H}_2\text{O}$  is most pronounced and the exact and approximate results

differ strongly within it. Other bands ( $\text{CH}_3\text{OH}$ ,  $\text{CO}$ ) are very weak in this case but their strength will be enhanced if the content of the corresponding component increases. In principle, the conclusions made about the behaviour of the efficiency factors and errors for silicate- $\text{H}_2\text{O}$  particles should be valid for other ices too.

As an example, we compared the extinction efficiency factors for homogeneous spheroids composed of pure  $\text{CO}$ . In our calculations, we used the refractive indices from the paper of Tielens et al. (1991) and tried to reproduce their Fig. 12 where the extinction profiles for spheroids in terms of the Rayleigh approximation are double-peaked. Indeed, in some cases the profiles have two peaks but their relative strengths and central positions are found to be strongly dependent on particle size and orientation.

The largest deviations between the exact solution and Rayleigh approximation within the  $\text{CO}$  profile do not exceed  $\Delta_{\text{ext}} \lesssim 3.8\%$ ,  $20\%$  and  $140\%$  if the particle size is  $r = 0.1 \mu\text{m}$ ,  $0.25 \mu\text{m}$  and  $0.5 \mu\text{m}$ , respectively. These values are larger than those for the silicate- $\text{H}_2\text{O}$  spheroids, but the calculations show that the errors may decrease by about a quarter for inhomogeneous spheroids with a small silicate core coated by a mantle of pure  $\text{CO}$  ice ( $V_{\text{core}}/V_{\text{total}} = 0.1$ ).

## 4. Conclusions

We investigated the accuracy of the Rayleigh approximation for coated spheroids in the case of modelling the absorption dusty bands in the near-infrared. The consideration has been performed in the wavelength range  $\lambda \lambda 2.7\text{--}22 \mu\text{m}$  for spheroids of different shape and structure with the sizes  $r$  up to  $1 \mu\text{m}$  ( $r$  is the radius of a sphere with the same volume as a spheroid).

It is found that for fixed chemical composition the error induced by the use of the Rayleigh approximation is mainly determined by particle size. Our principal results are as follows:

*Extinction:* The 10% accuracy can be reached if the size of particles  $r \lesssim 1.15 \mu\text{m}$ ,  $0.85 \mu\text{m}$  and  $0.25 \mu\text{m}$ , within the  $18 \mu\text{m}$ ,  $10 \mu\text{m}$  and  $3 \mu\text{m}$  bands, respectively.

*Polarization:* The same limit can be obtained for smaller grains:  $r \lesssim 1.10 \mu\text{m}$ ,  $0.35 \mu\text{m}$  and  $0.15 \mu\text{m}$  in the case of the  $18 \mu\text{m}$ ,  $10 \mu\text{m}$  and  $3 \mu\text{m}$  bands, respectively.

*Acknowledgements.* The authors are thankful to V.B. Il’in for critical reading of the manuscript and J.W. Hovenier, the referee, for many valuable comments. This work was supported by grants of the Volkswagen Foundation, the program “Astronomy” of the government of the Russian Federation and the program “Universities of Russia – Fundamental Researches” (grant N 2154).

## References

- Aitken D.K., Roche P.F., Smith C.H., et al., 1988, MNRAS 230, 629
- Aitken D.K., Smith C.H., Roche P.F., 1989, MNRAS 236, 919
- Bohren C.F., Huffman D.R., 1983, Absorption and scattering of light by small particles. John Wiley, New York
- Boogert A.C.A., Schutte W.A., Helmich F.P., et al., 1997, A&A 317, 929

- Draine B.T., Lee H.M., 1984, ApJ 285, 89  
Farafonov V.G. 1994, Opt. Spektrosc. 76, 79  
Farafonov V.G., Voshchinnikov N.V., 1997, Opt. Spektrosc. 83, 973  
Farafonov V.G., Voshchinnikov N.V., Somsikov V.V., 1996, Appl. Opt. 35, 5412  
Hough J.H., Whittet D.C.B., Sato S., et al., 1989, MNRAS 241, 71  
Hough J.H., Chrysostomou A., Messinger D., et al., 1996, ApJ 461, 902  
Hudgins D.M., Sandford S.A., Allamandola L.J., Tielens A.G.G.M., 1993, ApJS 86, 713  
Laor A., Draine B.T., 1993, ApJ 402, 441  
Lee H.M., Draine B.T., 1985, ApJ 290, 211  
O'Donnell J.E., 1994, ApJ 437, 262  
Palumbo M.E., Tielens A.G.G.M., Tokunaga A.T., 1995, ApJ 449, 674  
Tielens A.G.G.M., Tokunaga A.T., Geballe T.R., Baas F., 1991, ApJ 381, 181  
van de Hulst H.C., 1957, Light scattering by small particles. John Wiley, New York  
Whittet D.C.B., 1992, Dust in the galactic environments. Institute of Physics Publishing, New York  
Willner S.P., Gillett F.C., Herter T.L., et al., 1982, ApJ 253, 174